

Limits on deeply penetrating particles in the $> 10^{17}$ eV cosmic-ray flux

R. M. Baltrusaitis, G. L. Cassiday, J. W. Elbert, P. R. Gerhardy, E. C. Loh, Y. Mizumoto, P. Sokolsky, and D. Steck

Physics Department, University of Utah, Salt Lake City, Utah 84112

(Received 29 November 1985)

We report on a search for deeply penetrating particles in the $> 10^{17}$ eV cosmic-ray flux using the University of Utah Fly's Eye detector. No such events have been found in 6×10^6 sec of running time. We consequently set limits on the following: quark matter in the primary cosmic-ray flux, high-energy long-lived weakly interacting particles produced in proton-air interactions, such as τ 's; astrophysical neutrino flux; and other hypothetical high-energy weakly interacting components of the cosmic-ray flux such as photinos.

I. INTRODUCTION

We report on a search for deeply penetrating particles in the $> 10^{17}$ eV cosmic-ray flux. This search was performed using the University of Utah Fly's Eye detector, as part of its normal operation. No unusual deeply penetrating events have been found in 6×10^6 sec of running time.

We consider the following as candidate sources for such events: (1) metastable quark matter as part of the primary cosmic-ray flux, (2) τ 's and other long-lived particles of energy $> 10^{17}$ eV (> 0.1 EeV, where 1 EeV is 10^{18} eV) produced in the interaction of the primary cosmic-ray flux with the atmosphere, and (3) weakly interacting particles of astrophysical origin, such as neutrinos and photinos. In what follows, we consider the contribution of each possible source separately and set limits on its flux and/or production cross section.

II. THE DETECTOR

The Fly's Eye detector¹ is an array of 67 1.5-m-diameter mirrors each with twelve or fourteen phototubes located at the focal plane. Extensive air showers (EAS's) with $E > 10^{17}$ eV passing through the atmosphere near the detector generate sufficient nitrogen scintillation light to allow imaging of the shower by the phototubes. Phototubes whose direction vectors intercept the EAS axis receive scintillation light. A combination of tube-hit geometry and timing of the relative delay between hit tubes allows the complete geometrical reconstruction of the shower. The variables chosen to describe the geometry are θ , ϕ , and R_p , the zenith angle, azimuthal angle, and impact parameter, respectively. A typical shower geometry is shown in Fig. 1. The reconstruction accuracy depends on the total track length projected on the celestial sphere. For tracks with track length $> 50^\circ$, the errors in θ and R_p are typically $\Delta\theta \sim \pm 2^\circ$ and $\Delta R_p/R_p \sim 0.1$. The reconstruction algorithm and error estimation has been checked by examining a subset of the data where the EAS is visible in a second, smaller Fly's Eye composed of eight mirrors. The stereo reconstruction available for such events give additional constraints and confirms the ade-

quacy of monocular reconstruction and error estimation.

The total energy of the incoming shower is determined from the analysis of the pulse height of hit tubes in a calorimetric way. Since the total scintillation light observed by any tube is proportional to the total number of ionizing particles traversing the field of view of the tube, the pulse-height distribution can be converted to a size distribution. The total energy of the shower is then derived from the size of the shower at maximum or by integrating the size curve. Figure 2 shows a representative shower profile.

Since detection efficiency improves with increasing light output, very energetic EAS's are visible over a larger fiducial volume. Figure 3 shows the distribution of EAS energy versus R_p for all tracks detected. The maximum detectable R_p increases as a function of energy. At $E = 10^{19}$ eV (10 EeV) showers with $R_p = 20$ km are detectable, while for 10^{18} eV (1 EeV) the maximum R_p is 5 km. Note that the R_p cutoff is due both to the $\Delta\theta$ cut and to atmospheric attenuation length, which is 15 km at nitrogen scintillation wavelengths. The approximate fiducial volume in which EAS's are detected with good efficiency is then a cylinder of radius $R = R_p^{\max}$ and height of 15 km, centered on the Fly's Eye.

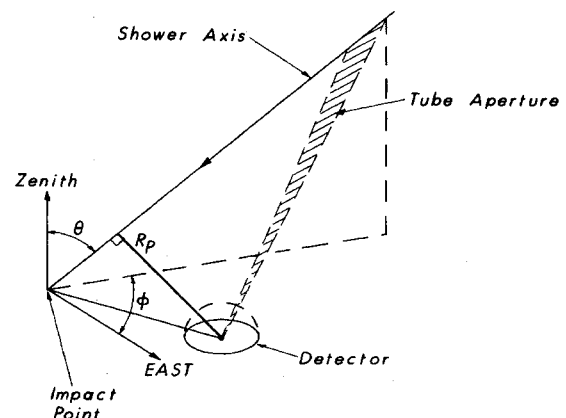


FIG. 1. Typical shower geometry.

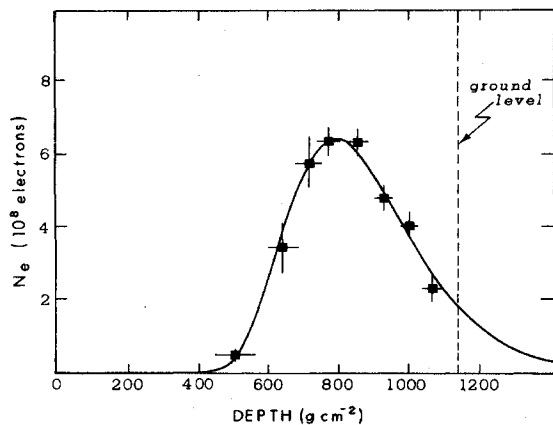


FIG. 2. Representative shower profile. The solid curve represents a fit using a Gaiser-Hillas [T. K. Gaisser and A. M. Hillas, in *Proceedings of the Fifteenth International Cosmic Ray Conference, Plovdiv, Bulgaria, 1977*, edited by B. Betev (Bulgarian Academy of Science, Sofia, Bulgaria, 1977)] parametrization for EAS development.

A by-product of the determination of shower profile is measurement of X_m , the depth of shower maximum in the atmosphere in g/cm^2 , and X_0 , the depth of first shower observation. This measurement allows us to estimate how many interaction lengths of atmosphere were traversed by the initial particle before interacting. The distribution of X_0 is shown in Fig. 4. Note that the X_0 distribution extends beyond the expected distribution of the actual point of first interaction since X_0 is always an upper limit on the actual interaction depth.

III. SEARCH PHILOSOPHY

We search for deeply penetrating (weakly interacting) particles in two ways. Observed EAS's with $\theta > 80^\circ$ typically must have traversed $> 3000 \text{ g}/\text{cm}^2$ of atmosphere before interacting. Since the interaction length of the atmosphere for protons is $\sim 45 \text{ g}/\text{cm}^2$ we expect to see no such events from normal hadronic interactions in our exposure time (see Fig. 5). Similarly, upward EAS's ($\theta > 90^\circ$) visible in our fiducial volume must originate in the Earth and hence must be produced by weakly interacting particles. We use downward events with $\theta > 80^\circ$ to set

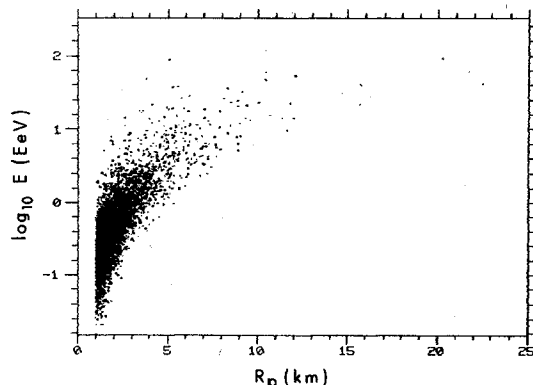


FIG. 3. Distribution of EAS energy versus R_p . 1 EeV is 10^{18} eV.

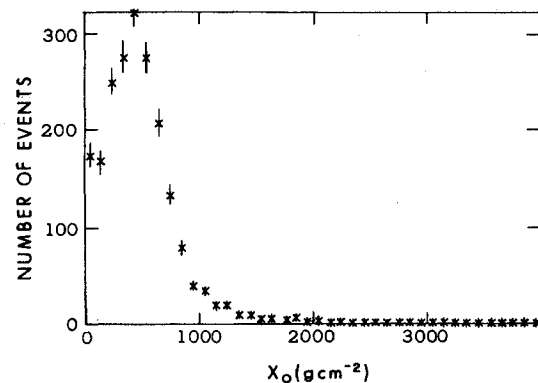


FIG. 4. Distribution of X_0 , the depth of first observed interaction of EAS.

limits on quark matter, on τ and τ -like particle production, and on the neutrino flux if the neutrino has an anomalously large interaction cross section ($\sigma_\nu \geq 10^{-31} \text{ cm}^2$). We also use downward events to set a limit on the flux times cross section for other hypothetical weakly interacting particles which might be present in the primary flux. Upward events are used to search for neutrinos with cross sections near those predicted by the standard model ($\sigma_\nu \sim 10^{-33} \text{ cm}^2$).

IV. QUARK-MATTER LIMITS

A number of authors³ have suggested the possibility of the existence of quark matter. This may be the absolutely stable ground state of QCD, it may decay rapidly, or it may be metastable. We consider the case where such quark matter is metastable in some region of baryon number $N_m > N_0 > N_c$. The production mechanism and mass and energy spectrum of such "globs" is unclear, but they may be formed in the early universe, in neutron stars, or in heavy nucleus collisions and may be an important component in the dark matter of the universe. It has been suggested that the "Centaurus" events observed at Mt. Chacaltaya can be interpreted as evidence for such objects.⁴

The metastability of such globs yields a straightforward prediction for their signature⁴ which we shall assume in what follows. It can be shown in various models that

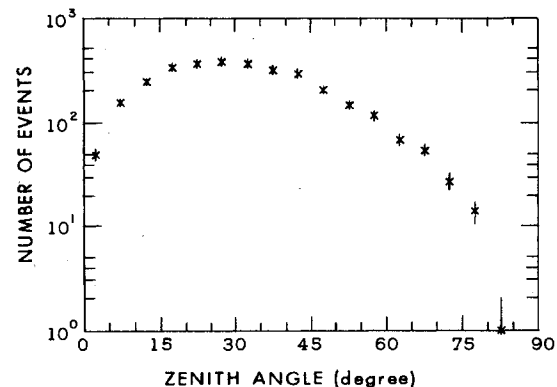


FIG. 5. Zenith-angle distribution of events.

TABLE I. Limits on quark-matter flux in the primary cosmic-ray spectrum in units of $(\text{cm}^2\text{secsr})^{-1}$. The 500-g/cm² point comes from Ref. 5.

Explosion depth (g/cm ²)	Explosion energy (eV)		
	10 ¹⁵	10 ¹⁸	10 ¹⁹
500	3×10^{-14}		
3000		1.4×10^{-18}	5.0×10^{-19}
4500		1.0×10^{-18}	1.6×10^{-19}
6000		1.2×10^{-18}	1.9×10^{-19}
7500		1.5×10^{-18}	2.4×10^{-19}
9000		1.8×10^{-18}	2.8×10^{-19}

such metastable objects become unstable when their baryon number drops below a critical value N_c . As such a glob traverses the atmosphere, it will be heated by collisions with air nuclei and lose energy by meson radiation or baryon evaporation. When the glob's baryon number decreases to N_c , it becomes unstable and explodes. The depth into the atmosphere of the explosion is given by

$$X \sim L_{\text{int}} \left[\frac{N_0 - N_c}{\Delta N} \right],$$

where L_{int} is the interaction length of the atmosphere (~ 30 g/cm² for globs of the radius of nitrogen) and ΔN is the mean baryon loss per collision. In this picture, quark-matter globs of a given baryon number N_0 will yield explosions at a given atmospheric depth, independent of initial energy (assuming they have not ranged out before exploding).

The energy loss before the explosion has been estimated to be a few percent of the glob energy per collision length. For $E_{\text{glob}} \sim 10^{19}$ eV, this would yield a continuous EAS from the top of the atmosphere of average size corresponding to the maximum size of a 10^{17} eV shower. This continuous energy loss would only be detectable at distance ≤ 2 km and is not presently used in estimating the Fly's Eye's sensitivity to such quark-matter globs.

We detect quark-matter globs by searching for EAS's as a result of glob explosions at depths X not accessible to ordinary hadronic events. The range of zenith angles

$80^\circ < \theta < 90^\circ$ yields depths of interaction in a fiducial volume $R \sim 5$ km (appropriate for explosion energies of $\sim 10^{18}$ eV) between 3000 and 10000 g/cm². No events have been observed with first visible depth $X_0 > 2500$ g/cm² (Fig. 4). Table I gives the resultant quark-matter flux limits as a function of explosion depth and explosion energy. The limits improve with the explosion energy because the effective fiducial volume increases. Also indicated for comparison are the flux limits derived by assuming that the Mt. Chacaltaya Centauro events are quark-matter explosions.⁵

We note that this flux limit for $X > 3000$ g/cm² is sensitive primarily to quark matter in the primary cosmic-ray flux, rather than to quark matter produced in the atmosphere. Quark matter, if it can be produced by the interaction of the heavy primary cosmic-ray component with the atmosphere (Fe-N interactions for instance), will have a maximum baryon number of 70 and, if ΔN is of order 1 and $L_{\text{int}} \sim 30$ g/cm², the glob will have exploded with $X < 2000$ g/cm², making it difficult to sort out from the tail of ordinary hadronic events.

V. LIMITS ON LONG-LIVED WEAKLY INTERACTING PARTICLE PRODUCTION

Hadronic decays of $> 10^{17}$ eV τ 's and τ -like particles produced in the interactions of the primary cosmic-ray flux with the atmosphere are a possible source of deeply penetrating downward EAS's. A τ produced with an energy of 10^{18} eV will have a $c\gamma\tau$ of ~ 50 km. Hence very distant cosmic-ray interactions, not themselves detectable by the Fly's Eye, could produce τ 's which penetrate into the Eye's fiducial volume and decay into observable EAS's. Since the cosmic-ray flux intensity for $10^{17} < E \leq 10^{19}$ eV is known,⁶ nonobservation of such events leads to a limit on the τ production cross section at $\sqrt{s} \geq 30$ TeV. Such a limit is of interest because it can lead to limits on heavy-quark production, since these can decay into τ 's. We also set limits on the production of τ -like particles as a function of their $c\gamma\tau$.

Since the minimum detectable τ energy is 10^{17} eV and the maximum primary cosmic-ray energy (E_p) with significant flux is 10^{19} eV, we are sensitive, with varying effi-

TABLE II. Limits on $(\sigma/\sigma_{\text{tot}})n(X)$ for weakly interacting particles produced in cosmic-ray-air interactions as a function of $c\gamma\tau$ and X .

E_p (eV) \ $c\gamma\tau$ (km)	50	100	200	500	1000
$X = 1$					
1.0×10^{17}	8.0×10^{-3}	3.0×10^{-3}	1.8×10^{-3}	1.6×10^{-3}	1.8×10^{-3}
4.0×10^{17}	4.0×10^{-2}	1.6×10^{-2}	1.0×10^{-2}	8.0×10^{-3}	1.0×10^{-2}
1.0×10^{18}	1.2×10^{-1}	5.0×10^{-2}	3.0×10^{-2}	2.6×10^{-2}	3.0×10^{-2}
1.0×10^{19}	8.3×10^{-1}	3.4×10^{-1}	2.0×10^{-1}	1.6×10^{-1}	1.8×10^{-1}
$X = 0.5$					
4×10^{17}	6.0×10^{-2}	2.4×10^{-2}	1.5×10^{-2}	1.2×10^{-2}	1.4×10^{-2}
1.0×10^{18}	1.8×10^{-1}	7.4×10^{-2}	4.6×10^{-2}	3.8×10^{-2}	4.2×10^{-2}
1.0×10^{19}		6.0×10^{-1}	3.6×10^{-1}	3.0×10^{-1}	3.6×10^{-1}
$X = 0.1$					
1.0×10^{18}		3.0×10^{-1}	2×10^{-1}	2×10^{-1}	2.6×10^{-1}

ciency, to $1.0 < X_\tau < 0.1$, where $X_\tau = E_\tau/E_p$. We note that many observations of hadronic charm production at accelerator energies have shown preferential large- X production.⁷ Hence the X region over which we are sensitive may be of interest even when softening effects due to decays into τ 's are taken into account.

The sensitivity to τ 's depends on the τ energy since this determines both the extent of the fiducial volume and the probability that the τ will decay within it. It also depends on the primary flux energy since the integral cosmic-ray flux $I(>E)$ falls as E^{-2} for $10^{17} \leq E \leq 10^{19}$ eV.

We calculate a limit on

$$[\sigma_\tau(E)/\sigma_{\text{tot}}(E)]n(X_\tau),$$

where $\sigma_\tau(E)/\sigma_{\text{tot}}(E)$ is the probability of producing a τ in cosmic-ray-air interactions and $n(X_\tau)$ is the normalized τ distribution function for such interactions. This limit is estimated in a Monte Carlo calculation where primary cosmic-ray interactions are generated in the upper atmosphere with our previously measured interaction distribution.² If the direction vector of the cosmic ray falls within the Fly's Eye fiducial volume, a τ with energy E_τ is generated and allowed to decay with decay length $c\gamma\tau$. We then keep track of whether the τ decay could have been detected by the Fly's Eye.

We write the total number of expected τ decays in the following simplified form:

$$N_\tau(E, E_\tau) = F(E)[\sigma_\tau/\sigma_{\text{tot}}]n(X_\tau)D(E_\tau) \\ \times \Delta(\Omega A(E_\tau))TB,$$

where $F(E)$ is the proton flux in $\text{cm}^2\text{sec sr}$, $D(E_\tau)$ is the probability of a τ of energy E_τ to decay in the fiducial volume, $\Delta(\Omega A(E_\tau))$ is the effective detector aperture for an EAS of energy E_τ , T is the total exposure time, and B is the τ branching ratio to hadrons and electrons.

Using this method, we find that the sensitivity to τ 's is maximized for primary energies between 10^{18} and 10^{19} eV and varies by approximately a factor of 2 in this interval. The limits on $(\sigma_\tau/\sigma_{\text{tot}})n(X_\tau)$ averaged over this energy interval for $x_\tau=1$ and $X_\tau=0.5$ are 5.4×10^{-2} and 1.8×10^{-1} , respectively. If the cosmic-ray flux at these energies is primarily composed of protons, we can set limits on $\sigma_\tau n(X_\tau)$ using our measured value of the p -air cross section of 520 mb^2 . We find $\sigma_\tau n(X_\tau)$ is less than 28 mb for $X_\tau=1$ and 94 mb for $X_\tau=0.5$.

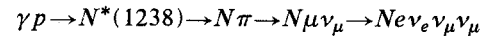
We generalize this search to include hypothetical weakly interacting particles produced in cosmic-ray-air interactions with decay lengths $20 \leq c\gamma\tau \leq 500 \text{ km}$. Since their mass is unknown, we cannot set limits on their lifetime directly. The only restriction on the nature of these particles is that they have interaction lengths $\gg c\gamma\tau$, and

that they decay into hadrons and/or electrons. We assume a branching ratio for such a decay of 0.5. Table II lists limits on their production probabilities as a function of their $c\gamma\tau$ and $X = E_x/E_p$, where E_x is the energy of the particle and E_p is the primary energy. Limits for $X=0.5$ range from 0.06 to 0.01 for $50 < c\gamma\tau < 500 \text{ km}$ at $E_p = 4 \times 10^{17} \text{ eV}$.

VI. LIMITS ON ULTRAHIGH-ENERGY NEUTRINO FLUX

We have recently reported⁸ limits on astrophysical neutrino fluxes at energies $> 10^{19}$ eV. Here we update these flux limits, extend them to lower energies, and describe the calculations in more detail.

The most intense expected source of $> 10^{17}$ eV neutrinos comes from the interaction of the primary cosmic-ray flux with the 2.7°K blackbody radiation. At proton energies of $> 10^{19}$ eV, the reaction



is above threshold for a significant fraction of 2.7°K photons. The onset of such a threshold implies a reduction in the mean free path for protons of energy $> 10^{19}$ eV and leads to the well-known prediction⁹ of a cutoff in the cosmic-ray flux at 5×10^{19} eV. A direct consequence is the existence of a flux of ν_μ 's and ν_e 's at $\geq 10^{17}$ eV in a ratio of 2 to 1. The contribution of neutrinos from atmospheric EAS's and other sources at these energies is expected to be many orders of magnitude below the contribution from this source. There have been several calculations of this effect with respect to both the primary-spectrum cutoff and the consequent neutrino flux.¹⁰ The flux expectations from various authors range from 10^{-17} to $10^{-18} \text{ } \nu/\text{cm}^2\text{sec sr}$ at $E_\nu = 10^{19}$ eV. The theoretical assumptions leading to this flux include (a) the universality and blackbody spectral shape of the 2.7°K radiation; (b) the universality, high-energy shape, and extent of source distribution and evolution of the primary cosmic-ray spectrum; and (c) the 300-MeV/ c photoproduction cross section and π and μ decay kinematics. Since (c) is well known, observation or nonobservation of such neutrinos test issues (a) and (b).

Contributions to the ultrahigh-energy (UHE) neutrino flux from point sources is possible but completely speculative. Weiler¹¹ has pointed out that if a substantial flux exists above 10^{21} eV, the reaction $\bar{\nu}_\tau \rightarrow Z^0$ can be used to search for the remnant neutrino flux. Observation of the neutrino flux from a highly red-shifted source would show an absorption dip at an energy $> 10^{20}$ eV which depends on the neutrino mass. This appears to be the only hope of directly measuring the relic neutrino background.

TABLE III. Limits of ν flux based on downward events ($\nu/\text{cm}^2(\text{sec sr})$).

E_ν (eV)	10^{17}	10^{18}	10^{19}	10^{20}
1×10^{-31}	1.0×10^{-14}	3.8×10^{-15}	1.0×10^{-16}	3.8×10^{-16}
1×10^{-30}	1.0×10^{-15}	3.8×10^{-16}	1.0×10^{-16}	3.8×10^{-17}
1×10^{-29}	1.0×10^{-16}	3.8×10^{-17}	1.0×10^{-17}	3.8×10^{-18}

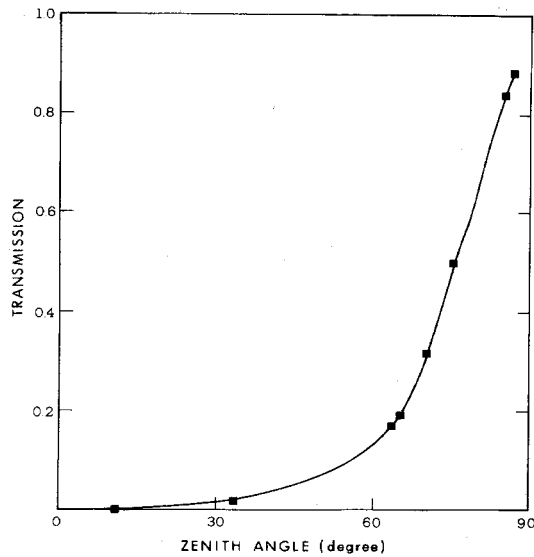


FIG. 6. Transmission of neutrino flux through the Earth as a function of zenith angle for $\sigma_\nu = 10^{-33} \text{ cm}^2$.

We search for the neutrino flux at energies $> 10^{20} \text{ eV}$ to examine the feasibility of this proposal as well as for the intrinsic interest in observing such high energy sources.

VII. NEUTRINO SIGNATURES

In the standard model for the reaction $\nu N \rightarrow \text{lepton} + X$, when $E_\nu \gg M_W c^2$, propagator effects distort the y distribution and $\langle y \rangle \rightarrow 0$. Hence, essentially all the energy in the ν interaction is expected to be transferred to the final-state lepton. We assume this to be the case at our energies. If we consider ν_e charged-current interactions only, the expected neutrino signature will thus be an EAS

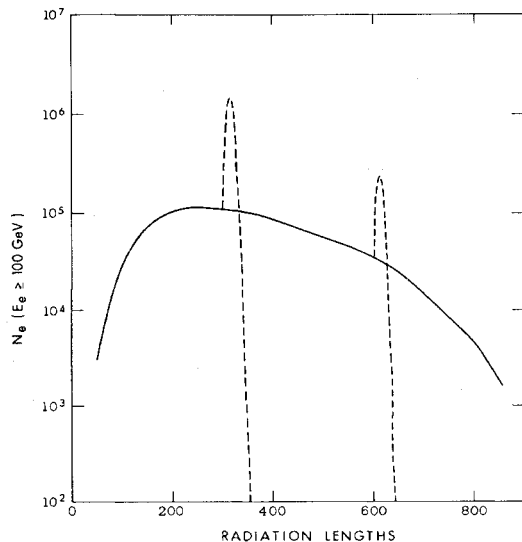


FIG. 7. Typical 10^{18} -eV crust-air-shower development. The solid curve represents the shower profile in the Earth's crust. The dashed curves indicate the profile in the atmosphere for a shower originating 300 and 600 radiation lengths into the crust. Electrons in the shower are followed to $E_e \geq 100 \text{ GeV}$.

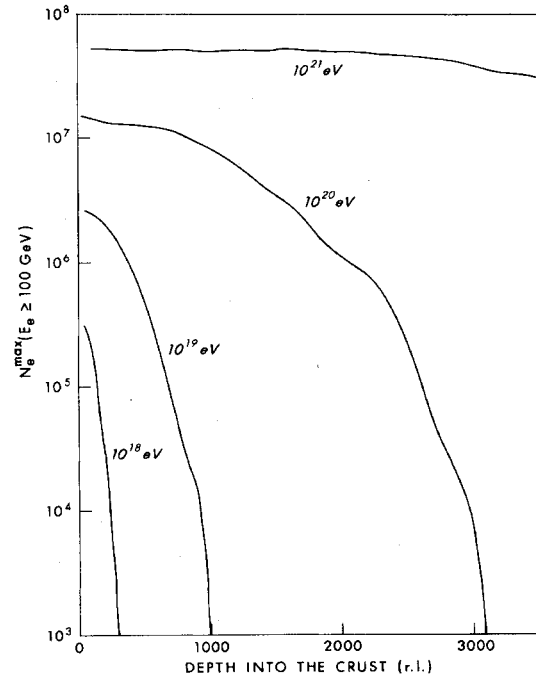


FIG. 8. Calculated shower size at shower maximum as a function of electron energy and depth of interaction in the crust.

produced by a $> 10^{17} \text{ eV}$ electron. However, electron and hadron showers of these energies are essentially indistinguishable by their profile in the atmosphere. The response and efficiency of the detector to such neutrino interactions is thus essentially identical to its response to hadronic cosmic rays. Hence our understanding of detector acceptance and efficiency based on our study of the hadronic cosmic-ray spectrum can be applied here.

Table III gives the flux limits based on no observed downward events with interaction point deeper than 2500 g/cm^2 . Note that the limits improve with increasing E_ν , because the fiducial volume increases. Limits approaching flux levels calculated by Hill and Schramm¹⁰ can only be achieved if σ_ν is orders of magnitude larger than predicted by the standard model. In particular, for $E_\nu = 10^{18} \text{ eV}$, Hill and Schramm predict a flux of $3 \times 10^{-16} \text{ v/cm}^2 \text{ sec sr}$. We can rule out such a flux only if σ_ν is greater than $1 \times 10^{-30} \text{ cm}^2$.

We can also set flux-times-cross-section limits on hypothetical, weakly interacting components of the primary cosmic-ray flux, such as photinos. The only requirements on such particles are that $\sigma_{\text{int}} < 10^{-29} \text{ cm}^2$ and that the final-state particles in the interaction carrying most of the energy be electrons, photons, and/or hadrons. Our data then imply a flux times cross section for such particles in units of $(\text{sec sr})^{-1}$ of 1×10^{-45} at 10^{17} eV to 3.9×10^{-47} at 10^{20} eV .

VIII. LIMIT BASED ON UPWARD EVENTS

Since particles producing upward events ($\theta_z > 90^\circ$) must travel through large numbers of interaction lengths of earth, there is no background from hadronic sources.

TABLE IV. Limits on ν flux based on upward events ($\nu/\text{cm}^2 \text{sec sr}$).

σ_ν (cm^2) \diagdown E_ν (eV)	10^{18}	10^{19}	10^{20}	10^{21}
10^{-33}	7.2×10^{-14}	9×10^{-15}	3.8×10^{-16}	5.0×10^{-17}
3×10^{-33}	1.4×10^{-13}	7.8×10^{-15}	7.2×10^{-16}	1.1×10^{-16}
5×10^{-33}	4.1×10^{-13}	2.3×10^{-14}	2.2×10^{-15}	3.3×10^{-16}
1×10^{-32}	3.7×10^{-12}	2.1×10^{-13}	2.0×10^{-14}	3.0×10^{-15}

Charged leptons will also be severely attenuated due to radiative energy losses, so that observation of upward events can be uniquely interpreted as observation of the UHE neutrino flux. The sensitivity to the neutrino flux is determined by two factors: (a) the attenuation of neutrinos by the Earth as a function of zenith angle, and (b) the depth into the Earth that a neutrino interaction can occur and still produce an atmospheric EAS sufficiently energetic to trigger the detector.

The attenuation length of the Earth is a function of the zenith angle since the average density of matter traversed by the neutrino depends on the depth of Earth's material sampled. We assume a density distribution for the Earth based on the Dziewonski-Anderson preliminary reference Earth model.¹² The resultant attenuation as a function of θ_z is shown in Fig. 6 for $\sigma_\nu = 10^{-33} \text{ cm}^2$. It is clear that the resultant angular distribution of events will peak near the horizontal direction.

Since we limit ourselves to the detection of the ν_e flux and most of the final-state energy is carried by the electron, the visible depth into the Earth is determined by the radiation length of earth.

For electron energies $> 10^{18}$ eV, the Landau-Pomeranchuk-Migdal¹³ effect becomes important and the pair-production and bremsstrahlung cross section are suppressed relative to the Bethe-Heitler cross section in dense materials. The effect is much less pronounced in the atmosphere.¹⁴ We have calculated, in a Monte Carlo program, the shower profiles of electrons produced in the Earth's crust ($\rho_{\text{crust}} = 2.6 \text{ g/cm}^3$) and entering the atmosphere ($\rho_{\text{atm}} \sim 10^{-3} \text{ g/cm}^3$). The net result is an elongation of the shower development while the shower is in the crust and a subsequent speed-up in development in the atmosphere (see Fig. 7). Since the Fly's Eye detection efficiency depends on the size of the atmospheric shower at maximum, we can estimate the detector's response to showers produced at different depths. Figure 8 shows the shower size at maximum as a function of E_ν and depth

into the crust. Showers are detected with good efficiency to depths of 40 m for $E_\nu = 10^{18}$, 100 m for $E_\nu = 10^{19}$, 300 m for $E_\nu = 10^{20}$, and 1200 m for $E_\nu = 10^{21}$ eV.

We quote flux limits (see Table IV) for upward events as a function of E_ν and σ_ν in the range 10^{-33} to 10^{-32} cm^2 . The standard model with $M_W = 80 \text{ GeV}/c^2$ predicts $\sigma_\nu \sim 10^{-33} \text{ cm}^2$. However, QCD effects may make this somewhat larger.¹⁵

IX. CONCLUSIONS

The ability of the Fly's Eye to determine the atmospheric depth of cosmic-ray interactions opens up a number of possibilities for searching for unusual particles in the primary flux such as quark matter and weakly interacting particles produced in the interactions of the cosmic-ray flux with the atmosphere. In addition, the present Fly's Eye has a sensitivity to upward going neutrino events approaching some recent predictions of the flux from cosmic-ray interactions with the 2.7 K blackbody radiation. Although some of these limits are not yet very restrictive, they are the first limits for such processes at these energies. We expect, as the sensitivity of the Fly's Eye improves and running time increases, that these limits will improve by an order of magnitude.

The limit on the neutrino flux above energies of 10^{21} eV of $< 5 \times 10^{-17}/\text{cm}^2 \text{sec sr}$ makes the search for relic neutrinos by the Weiler method extremely difficult, since a sizeable number of events would have to be collected to search for an absorption dip at some energy.

ACKNOWLEDGMENTS

The authors are grateful to Dr. Larry McLerran for discussions of quark-matter signatures. We gratefully acknowledge the United States National Science Foundation for providing the funds for the research.

¹R. M. Baltrusaitis *et al.*, Nuclear Instrum. Methods (to be published); R. Cady *et al.*, in *18th International Cosmic Ray Conference, Bangalore, India, 1983, Conference Papers*, edited by N. Durgaprasad *et al.* (Tata Institute of Fundamental Research, Bombay, 1983), Vol. 9, p. 351.

²R. M. Baltrusaitis *et al.*, Phys. Rev. Lett. **52**, 1380 (1984).

³T. D. Lee and G. C. Wick, Phys. Rev. D **9**, 2291 (1974); B. A. Freedman and L. D. McLerran, *ibid.* **16**, 1130 (1977); S. A. Chin and A. K. Kerman, Phys. Rev. Lett. **43**, 1292 (1979); A. K. Mann and H. Primakoff, Phys. Rev. D **22**, 1115 (1980); E. Witten, *ibid.* **30**, 272 (1984).

⁴J. D. Bjorken and L. D. McLerran, Phys. Rev. D **20**, 2353

(1979).

⁵Brazil-Japan collaboration, in *Proceedings of the Fifteenth International Conference on Cosmic Rays, Ploudiv, Bulgaria, 1977*, edited by B. Betev (Bulgarian Academy of Science, Sofia, 1977); D. Kazanas, V. K. Balasubrahmanyam, and R. E. Streitmatter, Phys. Lett. **142**, 23 (1984).

⁶B. Cady *et al.*, in *18th International Cosmic Ray Conference, Bangalore, India, Conference Papers* (Ref. 1), Vol. 9, p. 202.

⁷A. Kerman and G. VanDalen, Phys. Rep. **106**, 299 (1984).

⁸R. M. Baltrusaitis *et al.*, Astrophys. J. **281**, L9 (1984).

⁹K. Greisen, Phys. Rev. Lett. **16**, 748 (1966); V. A. Kuzmin and G. T. Zatsepin, Zh. Eksp. Teor. Fiz. **4**, 778 (1966).

- ¹⁰F. W. Stecker, *Phys. Rev. Lett.* **21**, 101 (1968); V. S. Berezinsky and G. T. Zatsepin, *Yad. Fiz.* **11**, 200 (1970) [*Sov. J. Nucl. Phys.* **11**, 111 (1970)]; S. H. Margolis, D. N. Schramm, and R. Silverberg, *Astrophys. J.* **221**, 990 (1978); F. W. Stecker, *ibid.* **228**, 919 (1979); C. T. Hill and D. N. Schramm, *Phys. Lett.* **131B**, 247 (1983); *Phys. Rev. D* **31**, 564 (1985).
- ¹¹T. Weiler, *Phys. Rev. Lett.* **49**, 234 (1982).
- ¹²T. L. Wilson, *Nature* **309**, 38 (1984); A. M. Dziewonski and D. L. Anderson, *Phys. Earth Planet. Inter.* **25**, 297 (1981).
- ¹³L. D. Landau and I. Ya. Pomeranchuk, *Dokl. Akad. Nauk SSSR* **92**, 535 (1953); A. B. Migdal, *Zh. Eksp. Teor. Fiz.* **32**, 633 (1957) [*Sov. Phys. JETP* **5**, 527 (1957)].
- ¹⁴E. Konishi, A. Misaki, and N. Fujimaki, *Nuovo Cimento* **44A**, 509 (1978).
- ¹⁵Yu. Andreyev, V. S. Berezinsky, and A. Yu. Smirnov, *Phys. Lett.* **84B**, 24 (1979).